Chiung-Wen Kuo[1]
Kung Hwa Wei[1]
Chun-Hsun Lin[2]
Jau-Ye Shiu[2]
Peilin Chen[2]

[1]Department of Material Science and Engineering, National Chiao Tung University, Hsin Chu, Taiwan
[2]Research Center for Applied Sciences, Academia Sinica, Taipei, Taiwan

Received December 26, 2007
Revised March 11, 2008
Accepted March 19, 2008

Research Article

Nanofluidic system for the studies of single DNA molecules

Here, we describe a simple and low-cost lithographic technique to fabricate size-controllable nanopillar arrays inside the microfluidic channels for the studies of single DNA molecules. In this approach, nanosphere lithography has been employed to grow a single layer of well-ordered close-packed colloidal crystals inside the microfluidic channels. The size of the polymeric colloidal nanoparticles could be trimmed by oxygen plasma treatment. These size-trimmed colloidal nanoparticles were then used as the etching mask in a deep etching process. As a result, well-ordered size-controllable nanopillar arrays could be fabricated inside the microfluidic channels. The gap distance between the nanopillars could be tuned between 20 and 80 nm allowing the formation of nanofluidic system where the behavior of a single λ-phage DNA molecule has been investigated. It was found that the λ-phage DNA molecule could be fully stretched in the nanofluidic system formed by nanopillars with 50 nm gap distance at a field of 50 V/cm.

Keywords:
Nanofluidic system / Nanostructures / Single molecule
DOI 10.1002/elps.200700943

1 Introduction

The size fractioning of biomolecules such as nucleic acids and proteins is one of the most important issues in the development of biotechnology. Conventional approaches for the separation of biomolecules rely on gel electrophoresis or gel filtration chromatography [1, 2]. However, the limited structure and size information of the gels prevented further optimization of the separation process, especially for the separation of large DNA molecules [3, 4]. To better understand gel electrophoresis, artificial gel structures have been developed using microfabrication techniques [5–8]. At the advent of single molecular imaging, it was possible to investigate the mechanical properties of single DNA molecules in artificial gel structures [9–11]. It has been observed that the motion of the DNA molecules in the restricted media would be directly influenced by their conformation states [12]. Since the DNA molecules are large biopolymers, the polymer will be constrained in the one or 2-D gel structures when the dimension of these structures is close to or smaller than the free solution diameter of a polymer. Therefore, it is important to investigate the behavior of single DNA molecules inside the artificial gel structures in order to optimize the performance of these gel structures. With the help of nanofabrication techniques, it has been demonstrated that the conformation of the DNA molecules could be manipulated in the designed nanostructures, such as nanochannels [13–17], nanopillars [18–23], and nanopores [24–26], to achieve effective separation of large biomolecules. However, the fabrication of nanostructures normally requires the expansive and time-consuming e-beam lithography [20, 21]. To explore the influence of the nanostructures on DNA molecules, it is desirable to develop an alternative simple and low-cost nanofabrication process for the nanofluidic system.

Recently, the colloidal particles have been utilized to construct 2-D and 3-D periodic nanostructures by the self-assembly process [27]. These well-ordered colloidal particles have been demonstrated capable of constructing nanofluidic system for the studies of single DNA molecules and the separation of large biomolecules [28–30]. In previous experiments, we have shown that it was possible to grow colloidal crystals at any desired area inside one- or 2-D microfluidic system using electrocapillary effect [31, 32]. Such type of self-assembled well-ordered nanostructures could be integrated into microfluidic system for the separation of large DNA molecules [33]. However, in these experiments the size tuning of the nanostructures was achieved by varying the size of nanoparticles, which was limited by the available sizes of the monodispersed nanoparticles. To investigate the influence of the nanostructures on the behavior of the DNA molecules, it is preferable to change the characteristic length of the nanofluidic devices systematically.

Here, we describe a simple technique to construct integrated periodic nanopillar arrays in the microfluidic system where the gap distance between the nanopillars can be tuned continuously. In this approach, nanosphere lithography [34]

Correspondence: Dr. Peilin Chen, Research Center for Applied Sciences, Academia Sinica, 128 Section 2, Academia Road, Nankang, Taipei 115, Taiwan
E-mail: peilin@gate.sinica.edu.tw
Fax: +886-2-27896680

has been employed to fabricate 2-D colloidal crystals at the desired area in the microfluidic channels. These colloidal crystals were then used as the etching mask for the nanopillar arrays in a deep etching process [35–38]. Since the polymeric nanoparticles were used in this experiment, the size of the nanoparticles could be trimmed by an oxygen plasma treatment. Therefore, the control of the gap distance between the nanopillars could be achieved systematically.

2 Materials and methods

2.1 Chip design and fabrication

To integrate nanostructures into the microfluidic system, we have adapted the design from a previous experiment [39] where two microchannels were connected by several channels with nanostructures as illustrated in Fig. 1. There are two main parts in this design: the sample injection/collection channels and the nanopillar array channels. In the injection channel, there are two inlets in the injection channels (A and B) and there are two outlets in the collection channels (C and D). The DNA sieving nanopillar array channels were composed of 32 parallel rectangular channels with 50 μm in width and 1 mm in length and separated from each other by 150 μm. The sieving channel was designed to confine the polystyrene nanoparticles to form single layer of well-ordered close-packed colloidal crystals, which served as the etching mask for the nanopillar arrays. To establish a uniform electrical field across the DNA sieving array channels, the negative driving voltage has been applied to both wells A and B to force the DNA molecules to travel through the nanopillar arrays before reaching wells C and D.

Figure 2 illustrates the fabrication process of the nanopillar array inside the microchannels using nanosphere lithography. In the first step, a standard n-type silicon (100) wafer (Gredmann) were first cut into 2.5×2.5 cm^2 pieces, and then cleaned with piranha solution (98% sulfuric acid and 30% hydrogen peroxide in the ratio of 3:1) under ultrasonic bath for about 20 min to remove the organic particles. After rinsing the chips several times with deionized (DI) water (18.2 MΩ, Millipore Simplicity) acetone and methanol solution, a standard photolithography and SPR 510A photoresist (Shipley, Marlborough, MA, USA) was used to create patterns for the nanopillar zone (Figs. 2a and b). Nanosphere lithography was then used to produce 2-D well-ordered close-packed structures in the nanopillar zone as shown in Fig. 2c. In this experiment, 580 nm monodispersed polystyrene beads (Bangs Laboratories, Fishers, IN, USA) were spin-coated on the chip. The polystyrene solution was prepared by adding 100 μL of colloidal particles into a dispersion solution (Triton X-100 in methanol 1:400). After the spin-coating process, well-ordered colloidal crystals in the nanopillar zone could be obtained, which then served as the etching mask for the nanopillar in a deep etching process. In order to control the gap distance between nanopillars, the polystyrene beads were trimmed by an oxygen plasma treatment (Oxford, Plasmalab 80 Plus, UK) with 20 sccm of oxygen at a pressure of 50 mTorr (Fig. 2d). These size-trimmed nanoparticles were then served as the etching mask in a deep etching process. To fabricate nanopillar arrays, a deep etching process has been employed using an induced coupled plasma etcher (STS MESC Multiplex ICP, UK). In each etching cycle, a "Bosch" process with two steps was used. In the etching step, the flow rate for SF_6 was 15 sccm and 2.0 sccm for O_2 gas and the etching time was 11.5 s at 600 W whereas in the passivation step the flow rate for C_4F_8 was 85 sccm and the time was 7.5 s at 600 W. Nanopillars with different aspect ratios could be produced by 5 to 20 cycles of etching process (Fig. 2e). After the deep etching process, the polystyrene beads and photoresist were removed by sonication of the sample in dichloromethane and acetone solution, respectively for 10 min. A second photolithographic process was used to create the patterns for the microfluidic channels connected to the nanopillar arrays (Fig. 2f). After another deep etching process, nanopillar arrays inside the microfluidic channels could be obtained (Fig. 2g). The microfluidic chip containing nanopillar arrays was then sealed with a cover slip (Fig. 2h). Before sealing with cover slip, the silicon substrates were mechanical drilled through the backside to access the inlets. To prevent electrical leakage, an oxide layer was thermally grown on the silicon substrates at 1100 °C for 2 h. The bonding of the silicon chip and the cover slip was achieved by spin coating a layer of silicone (PDMS) elastomer (RTV 615, General Electric, NY, USA) onto the cover slip. Both elastomer-coated cover slip and silicon substrate were pretreated with oxygen plasma (20 sccm, 100 mTorr and 100 W for 2 min) to enhance the surfaces wettability.

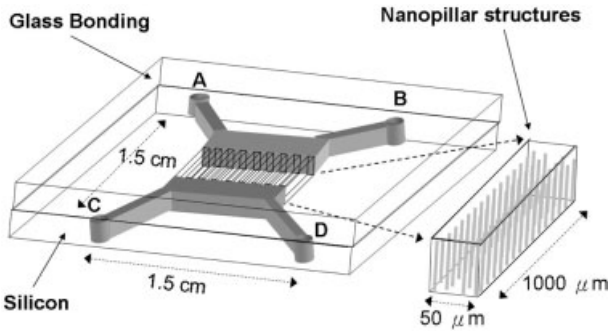

Figure 1. Conceptual design of nanopillars as the DNA sieving matrix in the integrated microfluidic chip.

2.2 DNA electrophoretic separation

To investigate the performance of the nanofluidic system formed by the nanopillar arrays, λ-phage DNA (MW 48.5 kbp, Sigma) was used in this experiment. The DNA molecules were labeled with YOYO-1 fluorescence dye (nucleic acid dye, trade name, Invitrigen, Carlsbad, CA,

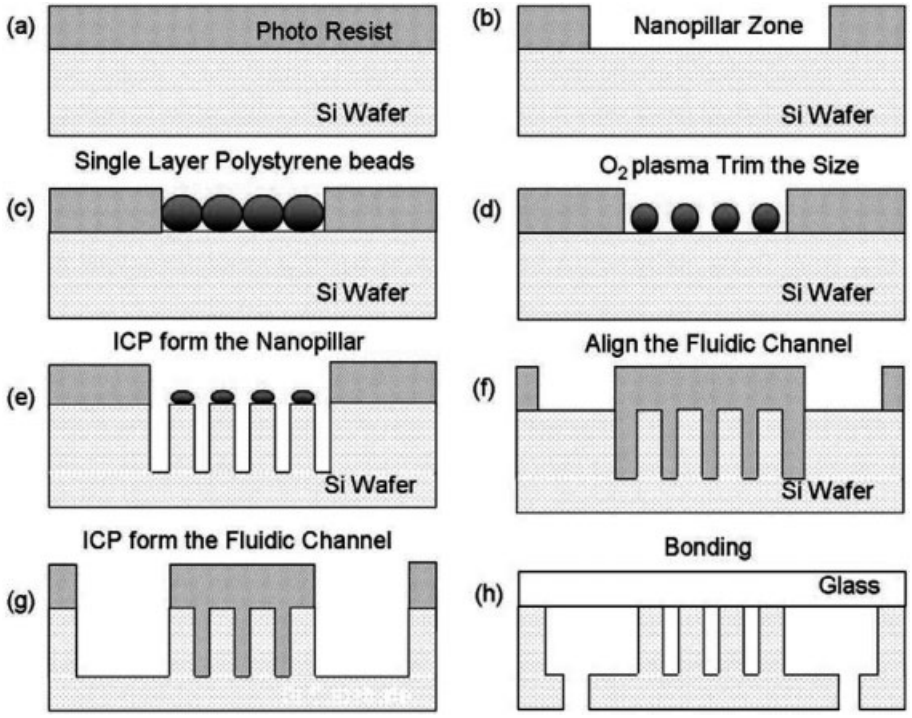

Figure 2. (a) and (b) Photolithography is used to create patterns for the nanopillar zone. (c) Nanosphere photolithography is used to produce closed-packed structures. (d) The size of nanosphere is trimmed by oxygen plasma treatment. (e) A deep etching process is used to fabricate nanopillar arrays. (f) and (g) Second etching process is used to create microfluidic system connected to nanopillar array. (h) Cover glass is bonded to a silicon wafer to form a nanofluidic system.

USA) at 5:1 ratio in 5 × Tris-borate-EDTA buffer (TBE, pH 8.0, Sigma–Aldrich). The final concentration of DNA solution was 0.5 μg/mL. The fluorescence images of the single λ-phage DNA molecules were captured by a cooled CCD camera (Cascade 512B, Roper Scientific, Duluth, GA, USA) mounted on an inverse microscope (IX71, Olympus, Japan) with a 60 × oil immerse lens. The trajectories of single λ-phage DNA molecules in the nanofluidic system were traced by Image-Pro software. To inject λ-phage DNA molecules into the channel, a drop of 5 × TBE buffer was pipetted into the inlet A and outlet C. The capillary force would fill the whole channel with TBE buffer. 10 μL of λ-phage DNA solution was then added into wells A and B and an electric field of 3 V/cm was used to move DNA molecule toward wells C and D by electrokinetic flow. The behavior of the single DNA molecules was investigated at different applied fields.

3 Results and discussion

3.1 Nanosphere lithography

Nanosphere lithography has been shown to be one of the simplest approaches to fabricate large-area nanostructures with sufficient size and shape control. It has been demonstrated that both 2-D and 3-D periodic nanostructure can be produced by the self-assembly process of the colloidal particles [32, 40]. These well-ordered nanostructures could be further used as templates for producing other nanomaterials, which could not form self-assembled structures by themselves. In this experiment, monodispersed polystyrene beads were spin-coated onto the solid substrates forming well-ordered 2-D arrays of colloidal crystals inside the microfluidic channels. These close-packed polystyrene beads were used as the etching mask for producing nanopillar arrays. The nanofluidic system could be constructed by forcing the fluid to go through the space between the nanopillars. Therefore, it was very important to control the spacing between nanopillars. In the conventional nanosphere lithography, the size control of the nanostructures was achieved by using nanoparticles with different diameters. However, the nanosphere lithography always produced close-packed structures where there was no space between nanopillars for the fluid to flow through.

In this experiment, the size control was achieved by oxygen plasma treatment. If nanoparticles were treated continuously with oxygen plasma, the relationship between the etching time and size of the nanoparticles was not linear. Therefore, a batch process was used. In each cycle, the nanoparticles were treated with 20 sccm of oxygen at a pressure of 50 mTorr and radio frequency (RF) power of 100 W for 30 s. Shown in Fig. 3 are SEM images of the size-trimmed nanoparticles in the microchannels at various treatment times. It can be clearly seen from these images that the gap distance between the nanoparticles can be systematically tuned by the oxygen plasma treatment. The measurement of the gap distance as a function of oxygen plasma treatment time is plotted in Fig. 4. Since the oxygen plasma treatment was not an isotropic process and the nanoparticles were spherical, the relationship between the cycle of oxygen treat-

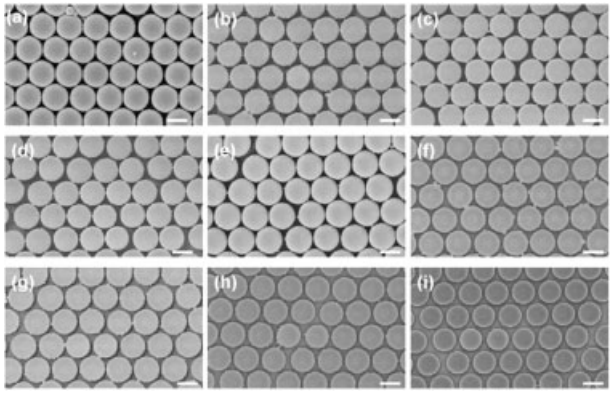

Figure 3. SEM images of the 580 nm polystyrene beads on silicon wafers treated by oxygen plasma. Oxygen plasma treatment time: (a) 0 s (b) 30 s (c) 60 s (d) 90 s (e) 120 s (f) 150 s(g) 180 s (h) 210 s (f) 240 s. All scale bars are 400 nm.

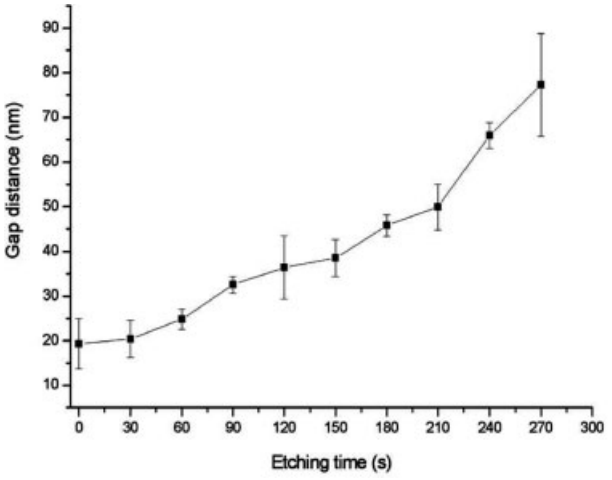

Figure 4. Relation between the oxygen plasma treatment time and the gap distance of the size-trimmed polystyrene beads as shown in Fig. 3.

ment and the gap distance was not linear as the number of cycle increased. However, the gap distance between nanopillars could still be tuned systematically between 20 to 80 nm.

3.2 Nanopillars in the microfluidic system

To fabricate nanopillar arrays in the microfluidic channel, the size trimmed nanoparticles in the nanopillar zone were used as the masks in a deep etching process. Shown in Fig. 5 are the SEM images of the nanopillars fabricated by different size trimmed polystyrene masks using a twenty-cycle "Bosch" process as described in Section 2. For the close-packed polystyrene beads (no oxygen plasma treatment), the deep etching process did not produce nanopillar structures because most area on the silicon substrate was masked by the polystyrene beads as shown in Fig. 5a. As the size of the polystyrene was reduced, nanopillars with different gap distances could be produced. Despite the fact that all the nanopillars shown in Fig. 5 were fabricated using twenty cycles of the deep etching process, the height of the nanopillars were different when different sizes of masks were used. The reason was that for the nanopillars with smaller gap distance, the substrate surface areas exposed to the plasma were smaller, therefore, reducing the etching efficiency.

One important issue in our process was to integrate the nanopillar arrays into microchannels, which was achieved by a second photolithographic and deep etching process. The top view and side view SEM images of the nanopillar arrays are displayed in Fig. 6. From Fig. 6 it can be seen that the nanopillar arrays are located inside the microfluidic channels. Since the nanosphere lithography is a self-assembly process, there are always some defects, such as point defects or line defects, in the close-packed structures as seen in Fig. 6a. These defects may trap some of the DNA molecules at a low flow rate. However, most of DNA molecules can easily escape from these defects at a moderate flow rate. In addition, the nanopillars can only be produced by single layer close-packed structures. A double layer of polystyrene beads would mask the etching process, which would produce nanopores instead of nanopillars. These nanopores can be seen at the edge of the microchannel in Fig. 6a. Since these nanopores are not connected, the fluid could not flow through these areas. Therefore, they would not change the flow pattern. To avoid the formation of double layer nanostructure, the thickness of the photoresist, which was used to confine the nanoparticles, should be smaller than the diameter of the polystyrene beads.

3.3 Sealing of the chips

The final stage for the fabrication of the nanofluidic chip was to seal the microfluidic channels so that the fluid could flow through the nanofluidic region confined by the nanopillar arrays. Two sealing techniques have been tested in this study. In the first trial an anodic bonding process [41] was used whereas an elastomer sealing [42–45] was investigated in the second test. Anodic bonding has been developed to fuse a silicon substrate to a glass under an applied voltage (500–1000 V) at an elevated temperature (300 to 600°C) for a few minutes. One advantage of using anodic bonding for sealing is that it is a direct bonding process without an additional insulator. However, it requires a very clean and smooth surface to active the interface functional group for the bonding process to take place. Since the anodic bonding is conducted at an elevated temperature, the coefficients of thermal expansion for these two materials should be roughly the same. Otherwise the stress developed in the cooling process will destroy the bonding formed at a higher temperature. In this experiment, a Pyrex 7740 glass (Corning, USA), which possessed a similar thermal expansion coefficient to the silicon substrate, has been used to seal the nanofluidic system

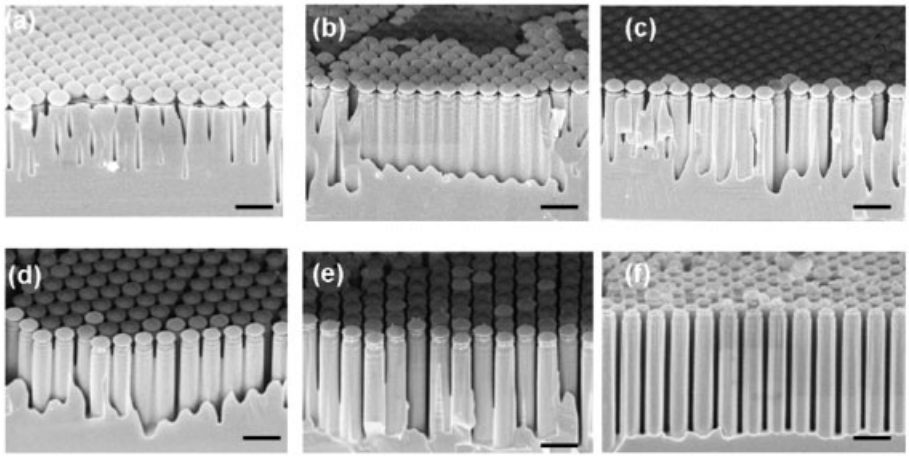

Figure 5. SEM images of the silicon nanopillars produced by a deep etching process using size-trimmed polystyrenes bead as the etching masks. The oxygen plasma treatment time for the polystyrene mask are (a) 0 s (b) 60 s (c) 90 s (d) 150 s (e)240 s (f) 270 s. All scale bars are 1 μm.

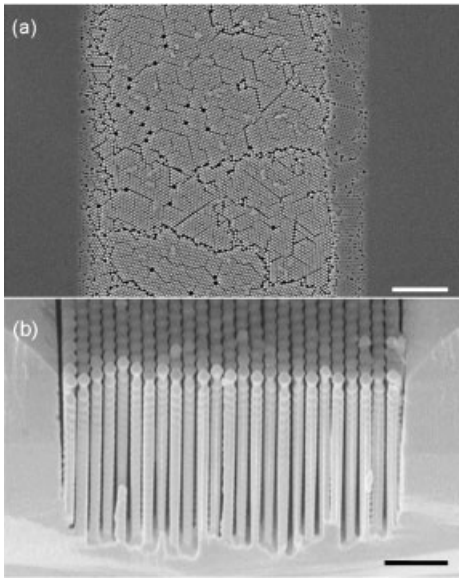

Figure 6. (a) Top view and (b) side view SEM images of the nanopillar arrays inside the microfluidic channel. The scale bar is 10 μm.

on the silicon substrate under the applied voltage of 850 V at 400°C for 15 min. The optical and the SEM images are displayed in Figs. 7a and b. From the SEM image, it was concluded that such boding process could be used to seal the silicon nanopillar array in the microchannels. However, the use of the special glass limited the application of such process.

In the second test, the bonding of the silicon chip and the cover slip was achieved by spin coating a layer of silicone (PDMS) elastomer (RTV 615, General Electrical, NY, USA) on the cover slip. Before bonding, both the elastomer-coated cover slip and the silicon substrate were pretreated with oxygen plasma, which rendered the surface hydrophilic. An irreversible bonding process took place when these two substrates were placed against each other. The SEM image of the elastomer sealed nanopillar array in the microchannel is shown in Fig. 7c. A good bonding was achieved by this process. Since there was no requirement for the substrates used in this bonding process, this sealing process could be used in many applications.

3.4 Single DNA molecules study

To examine the performance of the nanopillar arrays in the microchannel for the study of the behavior of single DNA molecules, a microfluidic system similar to that in Fig. 7a was used. In this system the channel height was about 900 nm and the gap distance between nanopillars was about 50 nm. YOYO-1 dye-labeled λ-phage DNA at a concentration of 0.5 μg/mL was pipetted into the inlet and injected into the microchannels using the protocol described in Section 2. The behavior of the single DNA molecules was investigated on an inverted microscope equipped with an EMCCD camera. Shown in Fig. 8 are the images of single DNA molecules moving in the nanofluidic system formed by nanopillar arrays at two different applied fields of 5 and 50 V/cm. Since the radius of gyration of λ-phage DNA was about 730 nm [24], the DNA molecules would be stretched when they flowed through the space between the nanopillars, which was about 50 nm. However, it was observed from the SEM image of the nanopillar array (Fig. 6a) that there existed some point defects in the nanopillar arrays, which might trap the DNA molecules. From Fig. 8a, it can be seen that at a low electric field, the DNA molecule underwent a stretch-recoil motion when they passed through the nanofluidic system. And the DNA molecule was trapped in a point defect as shown in frame 7–10. After some time, the trapped DNA molecule could escape from the defect and continued to move to the downstream. However, at a higher applied electric field of 50 V/cm, no trapped DNA molecules were observed. Most DNA molecules were stretched when they flowed through the nanopillar arrays. The maximum length of a stretched

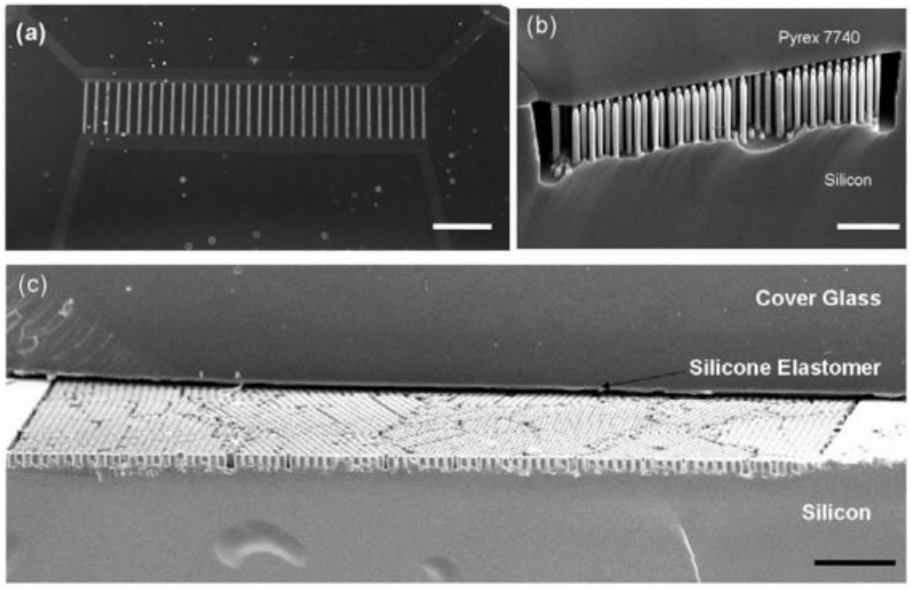

Figure 7. (a) Optical image of microfluidic chip with DNA sieving matrix. (b) The nanopillar array sealed by anodic bonding (850 V, 400°C for 15 min) with Pyrex 7740 glass. (c) Nanopillar array sealed by silicone elastomer. The scale bars are (a) 1 mm, (b) 4 μm, and (c) 5 μm.

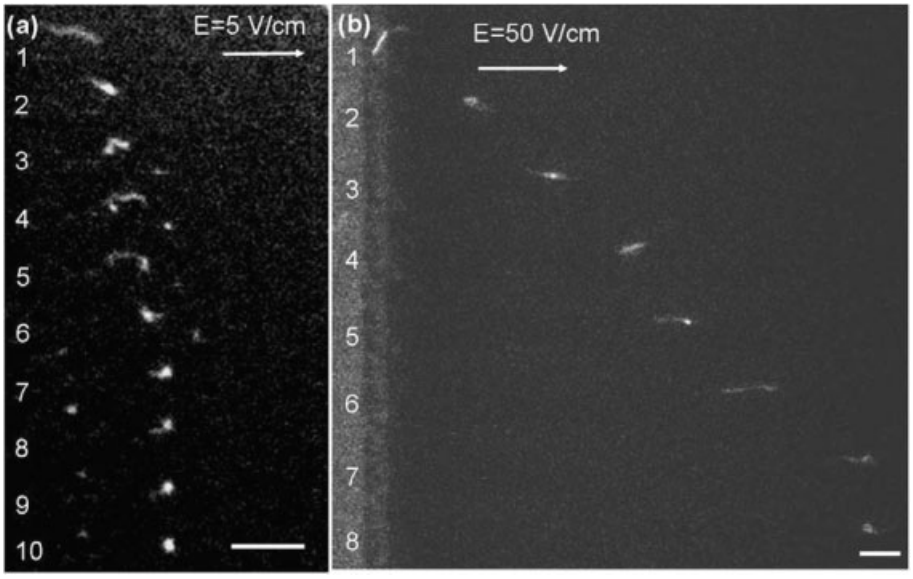

Figure 8. Time lapse images of λ-phage DNA inside the nanopillar with electric field of (a) 5 V/cm and (b) 50 V/cm. Elapsed time of each frame is 0.1 s. The scale bar is 10 μm. Concentration: 0.5 μg/mL.

DNA molecule was measured to be 16 μm, which corresponded to the contour length of λ-phage DNA. Therefore, we concluded that DNA molecules can be fully stretched in such nanofluidic system.

One important feature of this system was that it was possible to trace the trajectories of individual DNA molecules. Shown in Fig. 9 are the representative traces of the λ-phage DNA molecules at different applied fields. At low external field, the DNA molecules were found to be wondering around the nanopillar arrays. In this case, DNA molecules may be trapped in the defects. However, as the external field increased, the DNA molecules spent less time the nanopillar arrays. The defects did not play an important role in determining the trajectory of the DNA molecules. The mobility of the DNA molecules was calculated by averaging more than 20 trajectories of individual DNA molecules. The results are depicted in Fig. 10. The average mobility was about 3.5×10^{-4} cm^2/V·s, which was higher than those measured in other media. The origin of the high mobility measured in this system was not known at this time.

4 Concluding remarks

In summary, we have developed a low-cost large-scale fabrication technique to produce nanopillar arrays inside the microfluidic channel by size-tunable nanosphere litho-

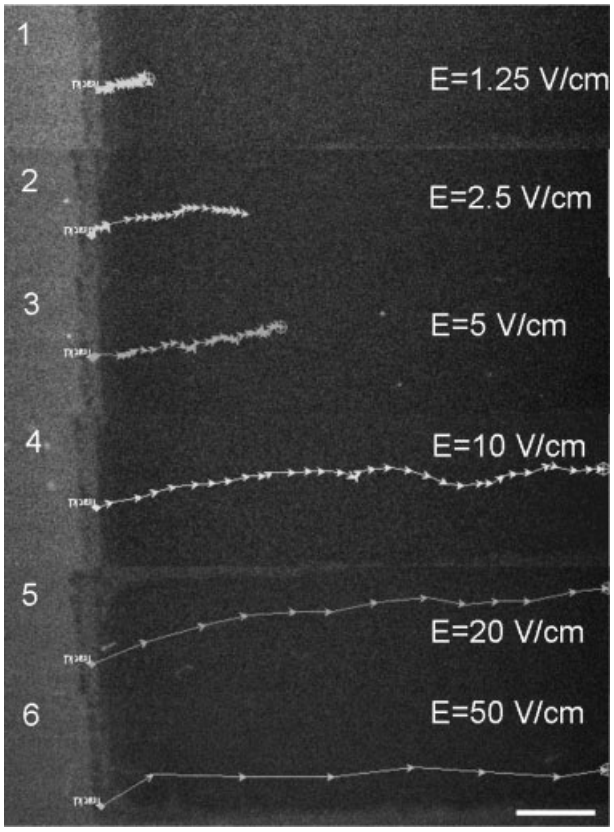

Figure 9. Trajectories of λ-phage DNA inside the nanopillar arrays at different applied field. The scale bar is 20 μm. Concentration: 0.5 μg/mL.

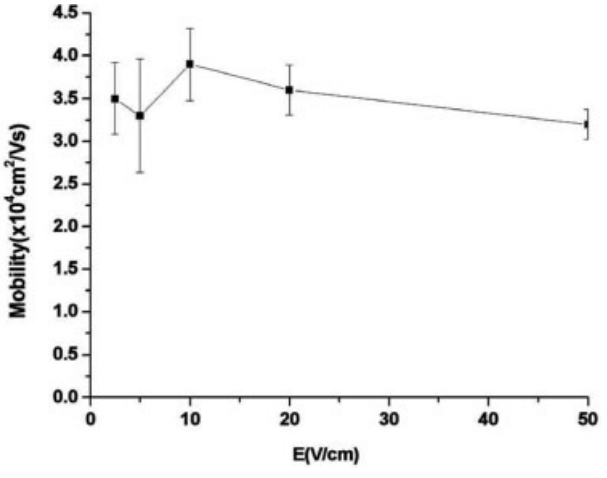

Figure 10. Electrophoretic mobility of λ-phage DNA as a function of the applied electric field.

graphy. By varying the oxygen plasma treatment time, the gap distance between the nanopillars could be tuned systematically from 20 to 80 nm. An elastomer bonding process was also introduced to seal the nanofluidic system with the cover slip. With the sealed nanopillar arrays it was possible to observe the electrophoretic behavior of individual DNA molecules inside the nanofluidic system. Therefore, it should be straightforward to construct integrated size-fractioning devices for biomolecules with the technique described here.

This research was supported in part by National Science Council, Taiwan under contract 96-2120-M-001-004 and Academia Sinica Research Project on Nanoscience and Technology.

The authors have declared no conflict of interest.

5 References

[1] Giddings, J. C., *Dynamics of Chromatography, Part 1, Principles and Theory,* Marcel Dekker, New York 1965.

[2] Scopes, R. K., *Protein Purification, Principles and Practice*, Springer-Verlag, New York 1993.

[3] Slater, G. W., Mayer, P., Drouin, G., *Methods Enzymol.* 1996, *270*, 272–295.

[4] Viovy, J. L., *Rev. Mod. Phys.* 2000, *72*, 813–872.

[5] Volkmuth, W. D., Austin, R. H., *Nature* 1992, *358*, 600–602.

[6] Volkmuth, W. D., Duke, T., Wu, M. C., Austin, R. H., Szabo, A., *Phys. Rev. Lett.* 1994, *72*, 2117–2120.

[7] Duke, T. A. J., Austin, R. H., Cox, E. C., Chan, S. S., *Electrophoresis* 1996, *17*, 1075–1079.

[8] Turner, S. W., Perez, A. M., Lopez, A., Craighead, H. G., *J. Vac. Sci. Technol. B* 1998, *16*, 3835–3840.

[9] Smith, S. B., Aldridge, P. K., Callis, J. B., *Science* 1989, *243*, 203–206.

[10] Han, J., Craighead, H. G., *Science* 2000, *288*, 1026–1029.

[11] Huang, L. R., Cox, E. C., Austin, R. H., Sturm, J. C., *Science* 2004, *304*, 987–990.

[12] Mandelkern, M., Elias, J. G., Eden, D., Crothers, D. M., *J. Mol. Biol.* 1981, *152*, 153–161.

[13] Cao, H., Tegenfeldt, J. O., Austin, R. H., Chou, S. Y., *Appl. Phys. Lett.* 2002, *81*, 3058–3060.

[14] Guo, L. J., Cheng, X., Chou, C. F., *Nano. Lett.* 2004, *4*, 69–73.

[15] Reccius, C. H., Mannion, J. T., Cross, J. D., Craighead, H. G., *Phys. Rev. Lett.* 2005, *95*, 268101.

[16] Mannion, J. T., Reccius, C. H., Cross, J. D., Craighead, H. G., *Biophys. J.* 2006, *90*, 4538–4545.

[17] Riehn, R., Austin, R. H., Sturm, J. C., *Nano Lett.* 2006, *6*, 1973–1976.

[18] Ohji, H., Izuo, S., French, P. J., Tsutsumi, K., *Sens. Actuators A Phys.* 2002, *97*, 744–748.

[19] Inatomi, K., Izuo, S., Lee, S. S., Ohji, H., Shiono, S., *Microelectron. Eng.* 2003, *70*, 13–18.

[20] Hattori, W., Someya, H., Baba, M., Kawaura, H., *J. Chromatogr. A* 2004, *1051*, 141–146.

[21] Kaji, N., Tezuka, Y., Takamura, Y., Ueda, M. *et al.*, *Anal. Chem.* 2004, *76*, 15–22.

[22] Chan, Y. C., Lee, Y. K., Zohar, Y., *J. Micromech. Microeng.* 2006, *16*, 699–707.

[23] Ogawa, R., Ogawa, H., Oki, A., Hashioka, S., Horiike, Y., *Thin Solid Films* 2007, *515*, 5167–5171.

[24] Nykypanchuk, D., Strey, H. H., Hoagland, D. A., *Science* 2002, *297*, 987–990.

[25] Zhang, H., Wirth, M. J., *Anal. Chem.* 2005, *77*, 1237–1242.

[26] Zeng, Y., Harrison, D. J., *Electrophoresis* 2006, *27*, 3747–3752.

[27] Jiang, P., Bertone, J. F., Hwang, K. S., Colvin, V. L., *Chem. Mater.* 1999, *11*, 2132–2140.

[28] Tabuchi, M., Ueda, M., Kaji, N., Yamasaki, Y. *et al.*, *Nat. Biotechnol.* 2004, *22*, 337–340.

[29] Zheng, S. P., Ross, E., Legg, M. A., Wirth, M. J., *J. Am. Chem. Soc.* 2006, *128*, 9016–9017.

[30] Zeng, Y., Harrison, D. J., *Anal. Chem.* 2007, *79*, 2289–2295.

[31] Shiu, J. Y., Kuo, C. W., Chen, P. L., *J. Am. Chem. Soc.* 2004, *126*, 8096–8097.

[32] Shiu, J. Y., Chen, P. L., *Adv. Mater.* 2005, *17*, 1866–1869.

[33] Kuo, C. W., Shiu, J. Y., Wei, K. H., Chen, P. L., *J. Chromatogr. A* 2007, *1162*, 175–179.

[34] Hulteen, J. C., Vanduyne, R. P., *J. Vac. Sci. Technol. A* 1995, *13*, 1553–1558.

[35] Kuo, C. W., Shiu, J. Y., Chen, P. L., *Chem. Mater.* 2003, *15*, 2917–2920.

[36] Kuo, C. W., Shiu, J. Y., Chen, P. L., Somorjai, G. A., *J. Phys. Chem. B* 2003, *107*, 9950–9953.

[37] Kuo, C. W., Shiu, J. Y., Cho, Y. H., Chen, P., *Adv. Mater.* 2003, *15*, 1065–1068.

[38] Cheung, C. L., Nikolic, R. J., Reinhardt, C. E., Wang, T. F., *Nanotechnology* 2006, *17*, 1339–1343.

[39] Tegenfeldt, J. O., Prinz, C., Cao, H., Chou, S. *et al.*, *Proc. Natl. Acad. Sci. USA* 2004, *101*, 10979–10983.

[40] Shiu, J. Y., Kuo, C. W., Chen, P. L., Mou, C. Y., *Chem. Mater.* 2004, *16*, 561–564.

[41] Wallis, G., Pomerant, Di., *J. Appl. Phys.* 1969, *40*, 3946–3949.

[42] Chou, C. F., Tegenfeldt, J. O., Bakajin, O., Chan, S. S. *et al.*, *Biophys. J.* 2002, *83*, 2170–2179.

[43] Chen, L., Ren, J., Bi, R. , Chen, D., *Electrophoresis* 2004, *25*, 914–921.

[44] Huang, X., Ren, J., *Electrophoresis* 2005, *26*, 3595–3601.

[45] Huang, X., Ren, *J. Trends Anal. Chem*. 2006, *25*, 155–166.

